CHIMIA **2023**, *77*, 417–423, https://doi.org/10.2533/chimia.2023.417

Supplementary Information

Late Microaerobic Growth for Efficient Production of Human Cytochrome P450 CYP3A4 in *E. coli*

Luca Marchetti, Matteo Planchestainer, Sven Panke, and Martin Held*

BPL, D-BSSE, ETH Zürich, Mattenstr. 26, Basel, CH-4058

Supplementary Materials and Methods

Feeding strategy (Fermentation IX)

To establish our feeding strategy, a preliminary test run operating a Minifors 2 reactor with the same settings as **VII** was performed. The only difference was the initial growth media (TB) composition, where we added 0.5 $g_{Glycerol}$ L^{-1} instead of 5 $g_{Glycerol}$ L^{-1} (10 % of the initially available carbon source).
90 min after inoculation, glycerol was fed at a linearly increasing rate $fr_{Test}(t)$ to account for the increase of biomass along the fermentation:

$$fr_{Test}(t) = \mathbf{0.013}\ g_{Glycerol}\ h^{-2} \cdot t + 0.019\ g_{Glycerol}\ h^{-1}$$

$fr_{Test}(t)$ was chosen to approximately match the estimated glycerol consumption rate $r_G(t)$ in the productive phase of **F VII**, which, due to biomass accumulation (0.2 gCDW h^{-1} in the productive phase), was time-dependent:

$$r_G(t) = 0.075\ g_{Glycerol}\ h^{-1}\ gCDW^{-1} \cdot 0.2\ gCDW\ h^{-1} \cdot t = \mathbf{0.015}\ g_{Glycerol}\ h^{-2} \cdot t$$

The glycerol concentration in the media remained constant at ~1 $g_{Glycerol}$ L^{-1}. However, under these conditions acetate levels increased reaching a final concentration of 10 $g_{Acetate}$ L^{-1} limiting cell growth to 4.7 gCDW L^{-1} compared to the batch process **VII** (6.2 gCDW L^{-1}) where peak values of 6.4 $g_{Acetate}$ L^{-1} were detected. The final volumetric yield was 343 $nmol_{CYP3A4}$ L^{-1} (72.9 $nmol_{CYP3A4}$ $gCDW^{-1}$), ~23% lower than for the batch process (**VII;** 446 $nmol_{CYP3A4}$ L^{-1}).

In experiment **IX**, we tried to modify the feeding strategy such that glycerol was supplied in sufficient amounts to maintain cell growth but not to accumulate in the media. Therefore, we regulated the feeding rate $fr_{\mathbf{IX}}(X)$ depending on the amount of formed biomass X:

$$fr_{\mathbf{IX}}(X) = 0.070\ g_{Glycerol}\ h^{-1}\ gCDW^{-1} \cdot X$$

The glycerol consumption rate observed in the productive phase of **VII** was 0.075 $g_{Glycerol}$ h^{-1} $gCDW^{-1}$. Using 0.070 $g_{Glycerol}$ h^{-1} $gCDW^{-1}$ we established a biomass dependent, slight underfeeding strategy (Figure S9A). The online cell density of the media during experiment IX was recorded using a turbidity sensor.

Assumption: 1 OD_{600} = 0.35 gram cell dry weight per liter (gCDW L^{-1})[1]

Eve® (Infors HT AG) script (C#-based) for turbidity dependent feeding pump regulation in fed-batch fermentation IX:

```
//variables and constants:
double V=0.7;                          // reaction volume [L]
double offset=7.7;                     // calibration turbidity/OD600nm (baseline)
double slope=2.36;                     // calibration turbidity/OD (slope)
double OD=0.35;                        // conversion OD -> gCDW
double r=70;                           // underestimated average glycerol conumption rate
                                       // (75 mg/h/gCDW) calculated from LAM_CYP3A4_17
double rho = 126;                      // density of the 10% (v/v) glycerol solution [g/L]
double m=r/rho;                        // feed volume per hour per gCDW per Liter [mL/h/gCDW]
double f = 2.52;                       // relationship % -> mL/h

double periodInMinutes = 0.5;          // update period of 30 seconds

// turbidity dependent feeding:
double density = (parameter.Turbidity.Value-offset)/slope * OD;
                                       // calculate density (gCDW/L) from turbidity signal

if (functionTime.TotalMinutes % periodInMinutes < 0.1)
                                       // within the last 6 seconds of the update period
{
output.Setpoint = density * m * V/f;  // update feeding pump setpoint
}
```

Plasmid details

pB233 b5 (pACYC184-backbone; 5.1 kbp):
(ori(p15A)-Ptac-Ptac-his tag-cyt b5-term-Cmp^R)

pB51 ompA-CYP3A4/*h*CPR (pCW-backbone, 9.7 kbp):
(M13 ori-Amp^R-ori(pBR322)-lacZ'-lac IQ-Ptac-Ptac-ompA-CYP3A4-Ptac-Ptac-pelB-*h*CPR)

Protein sequences

ompA-CYP3A4:

```
MKKTAIAIAVALAGFATVAQAAPMALIPDLAMETWLLLAVSLVLLYLYGTHSHGLFKKLGIPGPTPLPFLGNILSYHKGFCMF
DMECHKKYGKVWGFYDGQQPVLAITDPDMIKTVLVKECYSVFTNRRPFGPVGFMKSAISIAEDEEWKRLRSLLSPTFTSGKLK
EMVPIIAQYGDVLVRNLRREAETGKPVTLKDVFGAYSMDVITSTSFGVNIDSLNNPQDPFVENTKKLLRFDFLDPFFLSITVF
PFLIPILEVLNICVFPREVTNFLRKSVKRMKESRLEDTQKHRVDFLQLMIDSQNSKETESHKALSDLELVAQSIIFIFAGYET
TSSVLSFIMYELATHPDVQQKLQEEIDAVLPNKAPPTYDTVLQMEYLDMVVNETLRLFPIAMRLERVCKKDVEINGMFIPKGV
VVMIPSYALHRDPKYWTEPEKFLPERFSKKNKDNIDPYIYTPFGSGPRNCIGMRFALMNMKLALIRVLQNFSFKPCKETQIPL
KLSLGGLLQPEKPVVLKVESRDGTVSGA
```

pelB-*h*CPR:

```
MKYLLPTAAAGLLLLAAQPAMAMDIGSEFRNMGDSHVDTSSTVSEAVAEEVSLFSMTDMILFSLIVGLLTYWFLFRKKKEEVP
EFTKIQTLTSSVRESSFVEKMKKTGRNIIVFYGSQTGTAEEFANRLSKDAHRYGMRGMSADPEEYDLADLSSLPEIDNALVVF
CMATYGEGDPTDNAQDFYDWLQETDVDLSGVKFAVFGLGNKTYEHFNAMGKYVDKRLEQLGAQRIFELGLGDDDGNLEEDFIT
WREQFWPAVCEHFGVEATGEESSIRQYELVVHTDIDAAKVYMGEMGRLKSYENQKPPFDAKNPFLAAVTTNRKLNQGTERHLM
HLELDISDSKIRYESGDHVAVYPANDSALVNQLGKILGADLDVVMSLNNLDEESNKKHPFPCPTSYRTALTYYLDITNPPRTN
VLYELAQYASEPSEQELLRKMASSSGEGKELYLSWVVEARRHILAILQDCPSLRPPIDHLCELLPRLQARYYSIASSSKVHPN
SVHICAVVVEYETKAGRINKGVATNWLRAKEPAGENGGRALVPMFVRKSQFRLPFKATTPVIMVGPGTGVAPFIGFIQERAWL
RQQGKEVGRRCCTTAAAARMRTTCTGRSWRSSTGTVRSPSSTWPSPGSSPTRSTSSTC
```

CPR domain of P450$_{BM3}$ / BMR (*CYP102A1*):

```
TIKEMPQPKTFGELKNLPLLNTDKPVQALMKIADELGEIFKFEAPGRVTRYLSSQRLIKEACDESRFDKNLSQALKFVRDFAG
DGLFTSWTHEKNWKKAHNILLPSFSQQAMKGYHAMMVDIAVQLVQKWERLNADEHIEVPEDMTRLTLDTIGLCGFNYRFNSFY
RDQPHPFITSMVRALDEAMNKLQRANPDDPAYDENKRQFQEDIKVMNDLVDKIIADRKASGEQSDDLLTHMLNGKDPETGEPL
DDENIRYQIITFLIAGHETTSGLLSFALYFLVKNPHVLQKAAEEAARVLVDPVPSYKQVKQLKYVGMVLNEALRLWPTAPAFS
LYAKEDTVLGGEYPLEKGDELMVLIPQLHRDKTIWGDDVEEFRPERFENPSAIPQHAFKPFGNGQRACIGQQFALHEATLVLG
MMLKHFDFEDHTNYELDIKETLTLKPEGFVVKAKSKKIPLGGIPSPSTEQSAKKV
```

Reaction scheme NEN

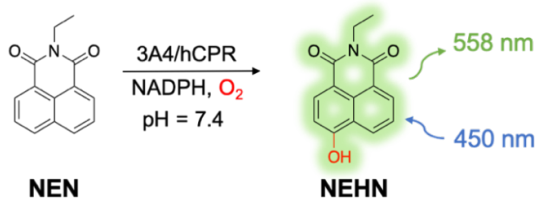

Scheme S1: **Reaction used for the quantification of CYP3A4 activity.** The reaction was carried out in *E. coli* lysates diluted in reaction buffer which were incubated with *N*-ethyl-1,8-naphtalinimide (NEN). The reaction was started by adding 200 µM NADPH.

Calibration curves

NEHN fluorescence/absorption calibration: NEHN was not commercially available as a standard for calibration. Calibration curves were therefore established by first fully converting fixed amounts of NEN (0 µM – 50 µM) in a standard reaction assay using CYP3A4 expressing cells harvested from bioreactor experiment **IV** (**Supplementary Table S1**). NEN was reacted by repeatedly adding 200 µM NADPH and fresh lysate to the reaction. The fluorescence and absorbance signals at $\lambda_{abs/ex}$ = 450 nm, λ_{em} = 550 nm, (Gain = 110) were monitored until the signals did not increase anymore upon further NEN/lysate supply (after the 3rd addition at 2.5 h). NEN depletion was confirmed by HPLC (<10 % NEN remaining). The final signal intensities were then used to fit a linear model for NEHN concentration *vs* signal calibration (**Supplementary Figure S1**). Fluorescence signal to concentration ratios were linear up to ~25 µM. Concentrations above this value were measured via absorbance at 450 nm.

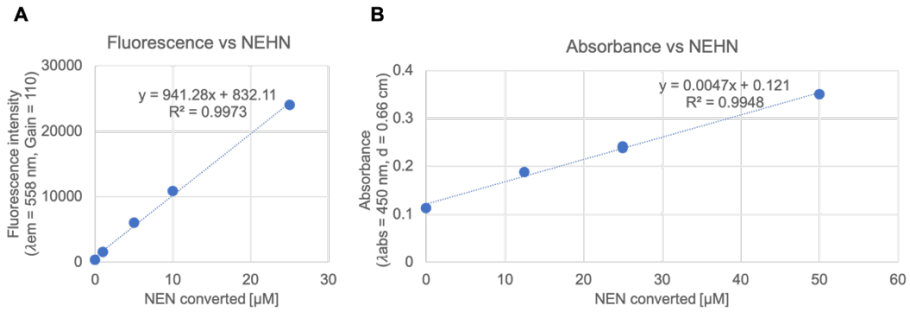

Supplementary Figure S1: NEHN calibration curves on the TECAN M1000 reader. To ensure total conversion of the substrate, 5x 200 µM as well as 5x 6 µL additional lysate were added over the course of 3 h. Additional NADPH or concentrated lysate did not change the signal over time, suggesting total conversion of NEN. **A)** Fluorescence signal ($\lambda_{abs/ex}$ = 450 nm, λ_{em} = 550 nm, Gain = 110). **B)** Absorbance (λ_{abs} = 450 nm, d = 0.66 cm).

Supplementary Results

Fermentation overview

Table S1: Overview over all fermentation experiments **I – IX**. AF: antifoaming agent added (y) or not (n). MF: MINIFORS fermenter (1 L working volume). MF2: MINIFORS 2 fermenter (0.7 L working volume). Yield: volumetric yield of functional CYP3A4 at the time of harvest. n.d.: not detectable (*average ± sd, n=2*)

ID	rpm [min^{-1}]	vvm [$L_{air}\ min^{-1}\ L^{-1}$]	DOT	volume [L]	k_La^{app} [h^{-1}]	mode	AF [y/n]	device	Harvest time [h]	Yield [$nmol_{CYP3A4}\ L^{-1}$]
I	variable	variable	10%	1	variable	batch	y	MF	14	**n.d.**
II	600	0.42	0 ↓ 95%	1	50	batch	y	MF	12	**n.d.**
III	300	3.6	0%	1	40	batch	y	MF	30	**399 ± 23**
IV	300	0.42	0%	1	16	batch	n	MF	42	**398 ±10**
V	100	0.42	0%	1	6	batch	y	MF	42	**185 ± 26**
VI	300	0	0%	1	0	batch	n	MF	42	**n.d.**
VII	400	0.42	0%	0.7	25	batch	n	MF2	40	**396 ± 2**
VIII	250	0.42	0%	0.7	8	batch	y	MF2	42	**110 ± 4**
IX	400	0.42	0%	0.7	25	fed-batch	n	MF2	42	**681 ± 50**

Shaking flask cultivation

Shaking flask cultivations were carried out in vented, non-baffled, conical 125 mL polycarbonate (PC) flasks at culture volumes of 50 mL (TB + Trace), 30 °C, shaking speeds of 200 rotations per minute (rpm) and shaking amplitudes of 25 mm. k_La^{app} values were calculated using the PreSens k_La^{app} Calculator tool[2]. Immediately after inoculation at an initial optical density at 600 nm (OD_{600}) of 0.02-0.1 from LB pre-cultures, the cells were induced with IPTG (0.1 mM) and 5-ALA (1 mM). The cultures were harvested after 24 h at 3'200 g for 10 min, washed once in KP_i wash buffer and stored at -20 °C.

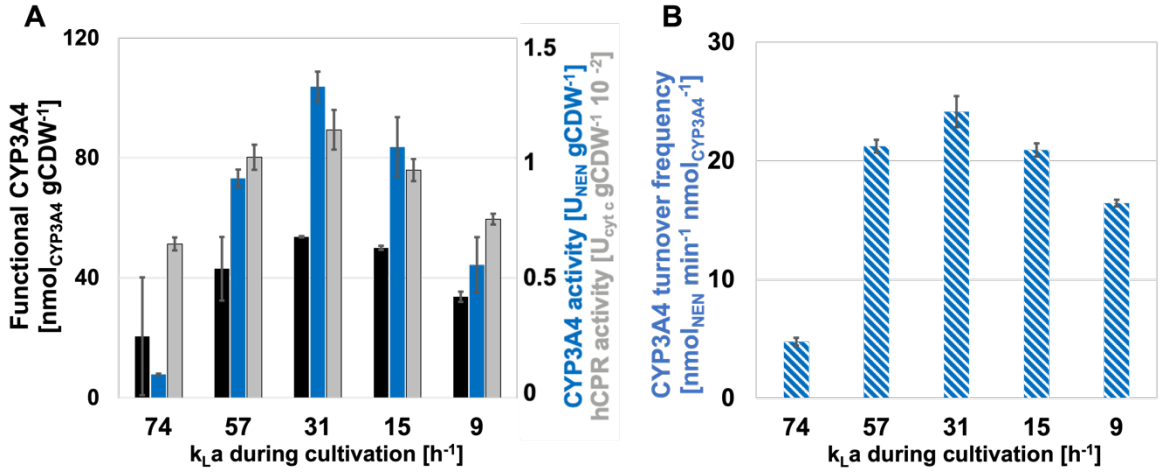

Figure S2: Cellular concentrations of functional CYP3A4 enzyme and activity of CYP3A4 and *h*CPR produced in shaking flasks. Activities were measured in lysates with 50 nM CYP3A4 (0.3-1.2 $mg_{Protein}\ mL^{-1}$). **A)** CYP3A4 produced per gCDW as measured by CO-binding (black bars), NEN conversion rates in lysates (blue bars) and *h*CPR activity in lysates (grey bars) *per* gCDW. **B)** turnover frequencies: $nmol_{NEN}\ min^{-1}\ nmol_{CYP3A4}^{-1}$ (*average with sd, n=3*)

Fermenter growth curves and CYP3A4 yields

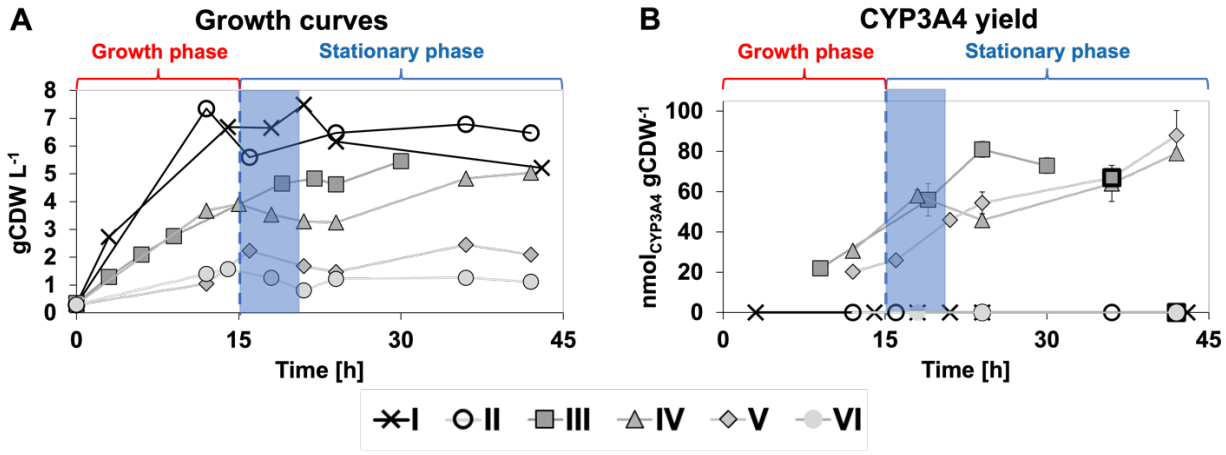

Figure S3: Growth curves and CYP3A4 production under microaerobic conditions in MINIFORS bioreactors (**I – IV**). **A)** Growth curves. Cell densities were calculated based on turbidity measurements at 600 nm using a conversion factor of 0.35 gCDW L^{-1} = 1 OD_{600nm}. **B)** Production of functional CYP3A4 as determined by CO-binding assay. The blue window approximately marks the most productive time of the late microaerobic processes (*average with sd, n=2*).

NEN conversion activity of enzymes produced by processes I – V over time

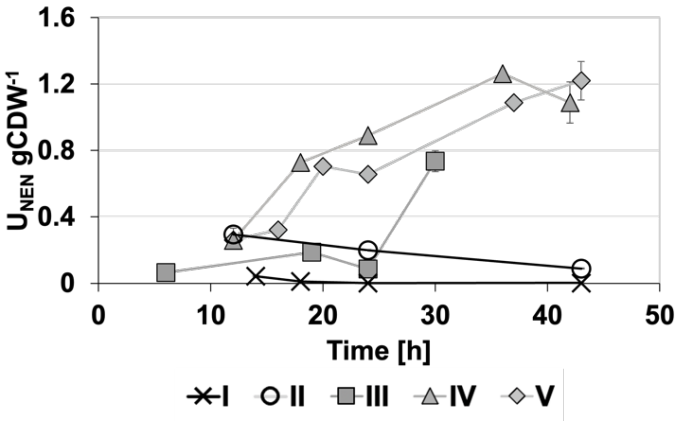

Figure S4: NEN conversion rates *per* gCDW over time (**I – V**). Whereas for microaerobic cultivation conditions (**I, II**) the activity measured per cell decreased steadily, the cells in late microaerobic experiments (**III – V**) became more active over time. (*average shown with sd, n = 3*)

CYP3A4 production in batch fermentations

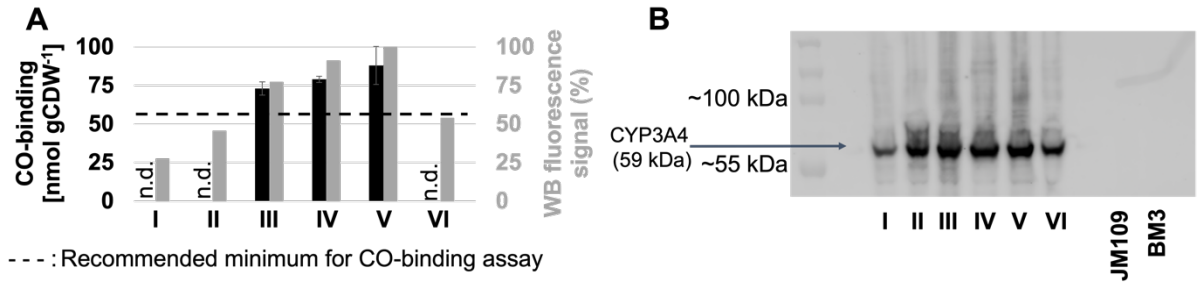

Figure S5: CYP3A4 production in batch fermentations across bioreactor experiments **I** – **VI** (shown are samples harvested at the following timepoints; I: 14 h, II: 12 h, III: 30 h, IV: 42 h, V: 42 h, VI: 42 h). **A)** CYP3A4 quantification by CO-binding (black bars) compared to relative western blot (WB) fluorescence signal intensities (grey bars; 100% represents the strongest signal). The dashed line (55 nmol $gCDW^{-1}$) corresponds to the lower limit of CYP concentrations in the CO-binding assay recommended by *Guengerich et al.*[3] (*average shown with sd, n = 2*) **B)** Western blot membrane of CYP3A4 visualized using monoclonal mouse anti-CYP3A4 primary antibody and infrared probe labelled goat anti-mouse secondary antibody (Li-Cor imager). Non-transformed *E. coli* JM109 wt cells and *E. coli* NEB cells expressing $P450_{BM3}$ grown in shaking flasks for 24 h are shown as negative controls. (n.d. = not detectable).

Enzyme stability assay

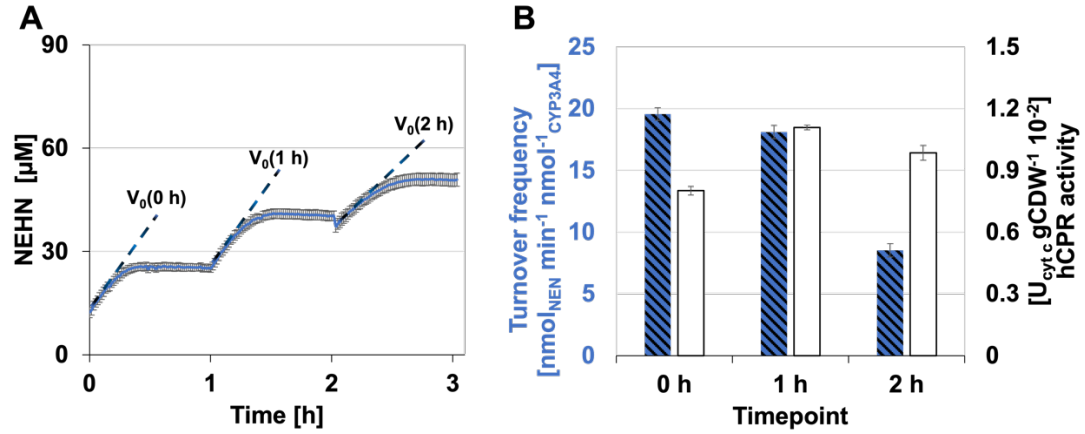

Figure S6: CYP3A4/*h*CPR stability assay. NEN conversion was performed in lysates from cells obtained from process **IV** after 42 h (k_La^{app} = 16 h^{-1}). **A**) NEHN formation measured by absorbance signal at λ_{abs} = 450 nm over time. The initial turnover rate was determined from the initial slope (5 min) after each spike. *h*CPR activity was determined by isolating and diluting 2 µL of the reaction mixture for a cytochrome c reduction assay. **B**) CYP3A4 turnover frequency and cell specific *h*CPR activities determined by NEN conversion and cytochrome c reduction assays. [CYP3A4] = 50 nM. (*average shown with sd*, *n = 3*)

CYP3A4 activity vs *h*CPR activity for flask and bioreactor

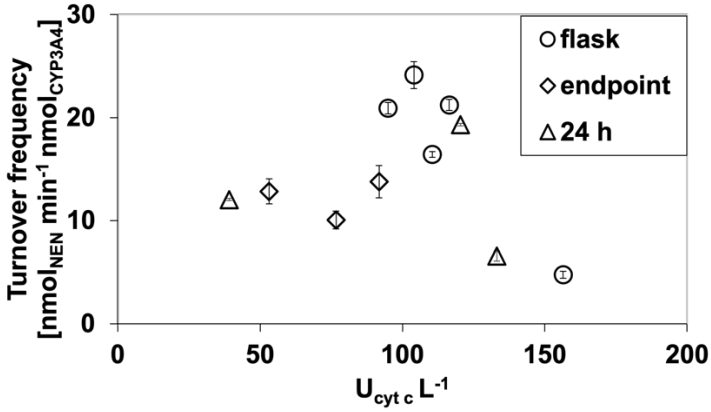

Figure S7: CYP3A4 turnover frequency *vs* *h*CPR activity. NEN-conversion per nmol$_{CYP3A4}$ measured by CO-binding (turnover frequency) for shake flasks and bioreactor experiments **I-VI** (after 24 h and at fermentation enpoints) *vs* cytochrome c reduction activity of *h*CPR per volume present during the NEN conversion assay (measured by cytochrome c reduction assay). [CYP3A4] = 50 nM. (*average shown with sd*, *n = 3*)

Late microaerobic batch cultivations VII and VIII

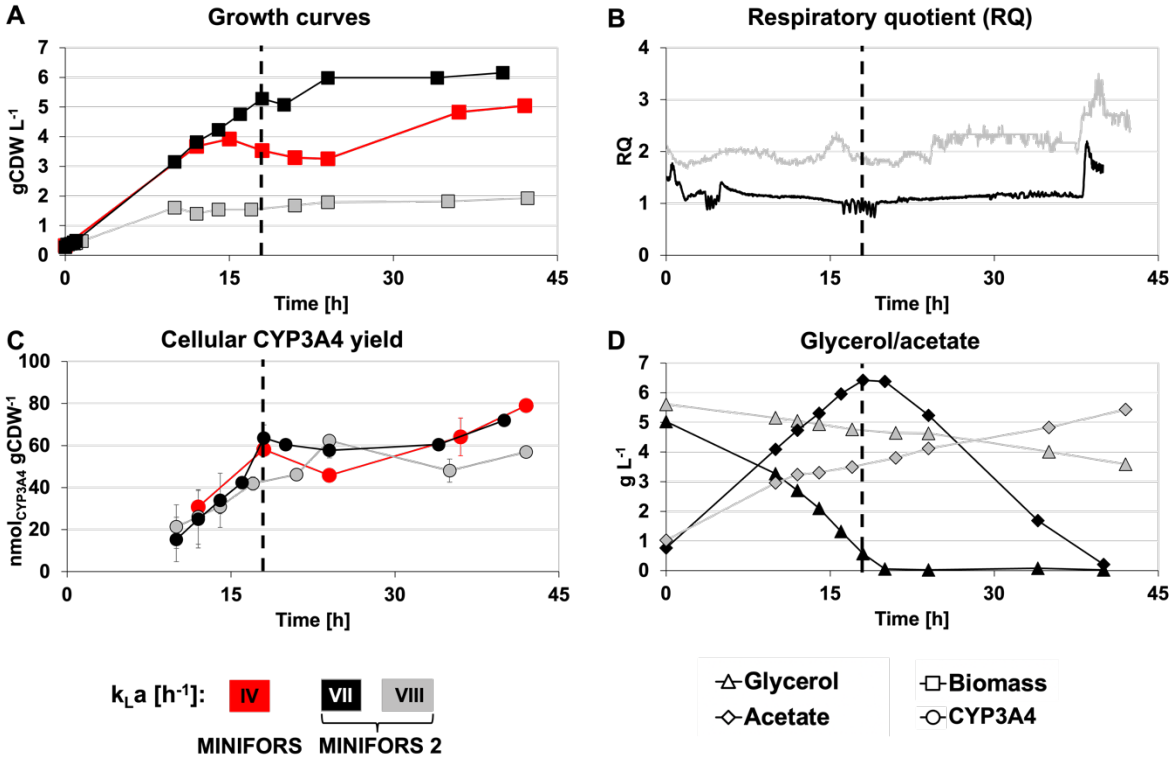

Figure S8: Late microaerobic batch cultivations **VII** and **VIII** of the CYP3A4 production strain **JM109**$^{CYP3A4/hCPR}$ in a MINIFORS 2 bioreactor. Comparison of two fermentations **VII** (k_La^{app} ~25 h^{-1}; black) *vs* **VIII** (k_La^{app} ~8 h^{-1}; grey). Late microaerobic fermentation **IV** (k_La^{app} ~16 h^{-1}; red) is displayed as a reference. **A)** Growth curves. Cell densities were calculated based on turbidity measurements at 600 nm using a conversion factor of 0.35 gCDW L^{-1} = 1 OD_{600}. **B)** Respiratory quotient (RQ). O_2 and CO_2 concentrations were measured with an off-gas sensor. **C)** Cellular CYP3A4 content was measured by CO-binding (*average with sd, n=2*). **D)** Glycerol and acetate concentrations in the culture media were determined by HPLC (RID).

Late microaerobic fed-batch cultivation IX *vs* batch process VII

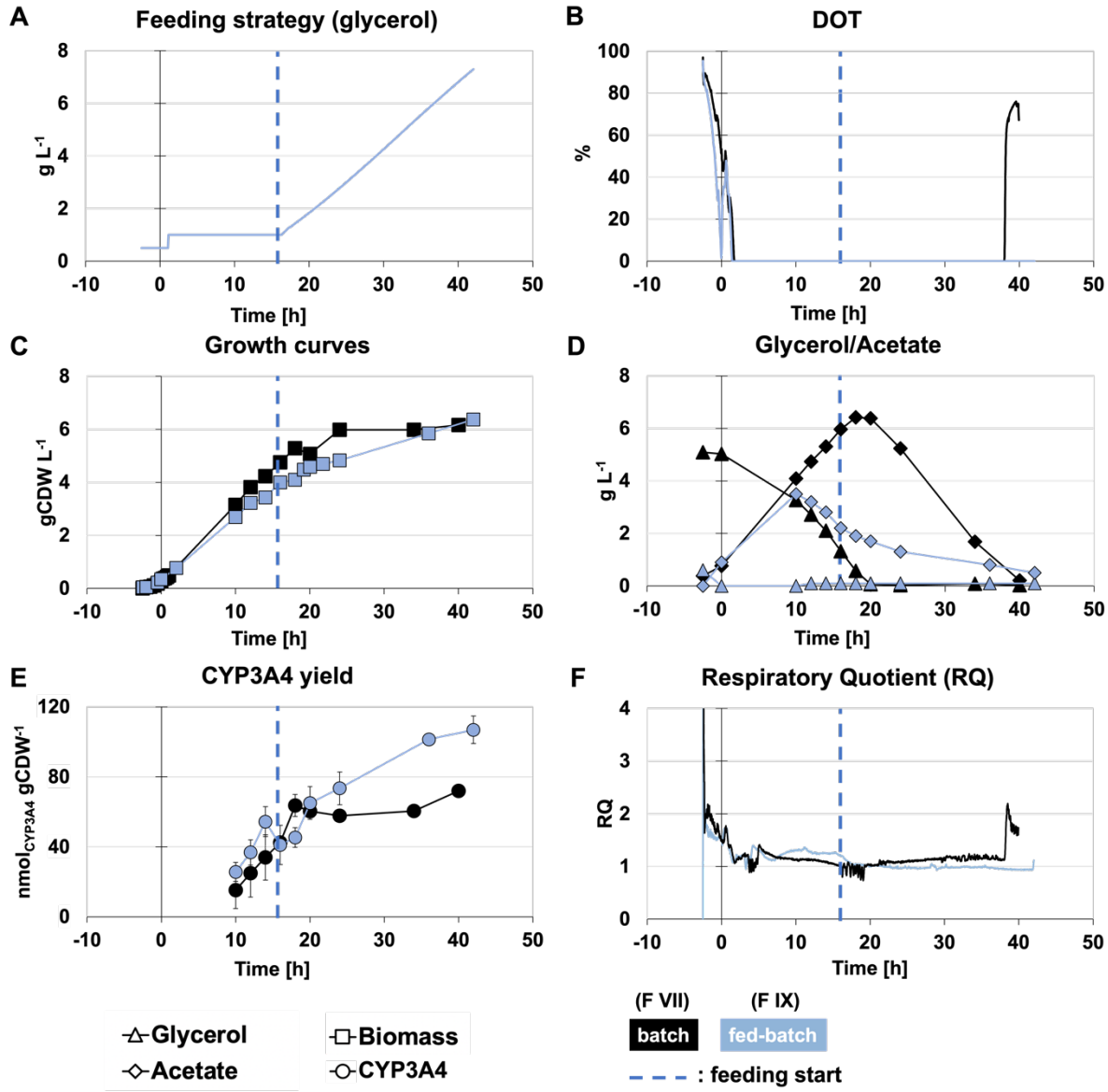

Figure S9: Late microaerobic batch cultivations **VII** and **IX** of the production strain **JM109**$^{CYP3A4/hCPR}$ in a MINIFORS 2 bioreactor. Comparison of two fermentations **VII** (k_La^{app} ~25 h^{-1}; black) *vs* **IX** (k_La^{app} ~25 h^{-1}; blue). **A)** Glycerol feed profile. The dashed blue line indicates the beginning of the fed-batch phase. **B)** Dissolved oxygen tension (DOT) profile. **C)** Growth curves. Cell densities were calculated based on turbidity measurements at 600 nm using a conversion factor of 0.35 gCDW L^{-1} = 1 OD_{600}. **D**) Glycerol and acetate concentrations in the culture media were determined by HPLC. **E)** Cellular ompA-CYP3A4 content was measured by CO-binding. (*average with sd, n=2*). **F)** Respiratory quotient (RQ). O_2 and CO_2 concentrations were measured with an off-gas sensor.

References

[1] F. Gong, G. Liu, X. Zhai, J. Zhou, Z. Cai, Y. Li, *Biotechnol. Biofuels* **2015**, *8*, 86, DOI: 10.1186/s13068-015-0268-1.

[2] kLa Calculator Tool, *https://www.presens.de/support-services/kla-calculator*, accessed May 6, **2023**.

[3] F. P. Guengerich, M. V. Martin, C. D. Sohl, Q. Cheng, *Nat. Protoc.* **2009**, *4*, 1245, DOI: 10.1038/nprot.2009.121.